

# Infrared Properties of Electron Doped Cuprates: Tracking Normal State Gaps and Quantum Critical Behavior in $\text{Pr}_{2-x}\text{Ce}_x\text{CuO}_4$

A. Zimmers,<sup>1</sup> J.M. Tomczak,<sup>1</sup> R.P.S.M. Lobo,<sup>1,\*</sup> N. Bontemps,<sup>1</sup> C.P. Hill,<sup>2</sup>  
M.C. Barr,<sup>2</sup> Y. Dagan,<sup>2</sup> R.L. Greene,<sup>2</sup> A.J. Millis,<sup>3</sup> and C.C. Homes<sup>4</sup>

<sup>1</sup>*Laboratoire de Physique du Solide (UPR 5 CNRS) ESPCI, 10 rue Vauquelin 75231 Paris, France.*

<sup>2</sup>*Center for Superconductivity Research, Department of Physics,  
University of Maryland, College Park, Maryland 20742, USA.*

<sup>3</sup>*Physics Department, Columbia University, New York, New York 10027, USA.*

<sup>4</sup>*Department of Physics, Brookhaven National Laboratory, Upton, New York 11973, USA.*

(Dated: October 4, 2018)

We report the temperature dependence of the infrared-visible conductivity of  $\text{Pr}_{2-x}\text{Ce}_x\text{CuO}_4$  thin films. When varying the doping from a non-superconducting film ( $x = 0.11$ ) to a superconducting overdoped film ( $x = 0.17$ ), we observe, up to optimal doping ( $x = 0.15$ ), a *partial* gap opening. A model combining a spin density wave gap and a frequency and temperature dependent self energy reproduces our data reasonably well. The magnitude of this gap extrapolates to zero for  $x \sim 0.17$  indicating the coexistence of magnetism and superconductivity in this material and the existence of a quantum critical point at this Ce concentration.

PACS numbers: 74.25.Gz, 74.72.Jt, 75.30.Fv, 75.40.-s

Over the last 15 years significant work has been done on the differences and similarities between electron and hole-doped cuprates [1]. The two material families share a structure with  $\text{CuO}_2$  planes, both exhibit superconductivity in a moderate doping range with  $\sim 0.16$  carriers per Copper, and both exhibit anomalous ‘normal’ (non-superconducting) states characterized in some doping and temperature ranges by a normal state gap or ‘pseudogap’.

In hole-doped materials early evidence for a ‘pseudogap’ came from nuclear magnetic resonance experiments [2, 3]. Angle-resolved photoemission (ARPES) experiments performed on the Bi-2212 material show that the pseudogap opens along the  $(0, \pi)$  direction in  $k$  space [4] and evolves smoothly into the superconducting gap as the temperature  $T$  is lowered. However, in the hole-doped materials gap-like features do not appear in the the optical conductivity and the pseudogap is only related to a sharp decrease in the optically defined scattering rate [5] instead of an upward shift in spectral weight for a density wave gap [6].

On the electron-doped side, the most studied material is  $\text{Nd}_{2-x}\text{Ce}_x\text{CuO}_4$  (NCCO) [7, 8]. The optical conductivity of non superconducting single crystals ( $x = 0$  to 0.125) shows the opening of a high energy “pseudogap” at temperatures well above the  $T_{Nee}$  associated with antiferromagnetic ordering [9]. ARPES measurements mapping the Fermi surface at low temperature for  $x = 0.04$ , 0.10 and 0.15 suggest the presence of pockets, as expected from long ranged magnetic order. For  $x = 0.15$  intensity is suppressed where the nominal Fermi surface crosses the magnetic Brillouin zone boundary [10].

In this Letter we report measurements of the temperature evolution of the optical conductivity in a set of  $\text{Pr}_{2-x}\text{Ce}_x\text{CuO}_4$  (PCCO) thin films. The PCCO mate-

rial has a wider superconducting range than does NCCO. Thin films are extremely homogeneous in the Ce concentration and are easier to anneal than crystals. Most important they can be made superconducting in the underdoped regime, whereas this seems difficult for crystals [9]. Our new generation of films are large enough to allow accurate optical studies, enabling us to track the optical behavior to lower energy scales and into the superconducting state [11]. Our data reveals the onset of a “high energy” partial gap below a characteristic temperature  $T_W$  which evolves with doping. The gap is directly evident in the measured optical conductivity for  $x = 0.11$  and 0.13, it is absent down to 5 K for  $x = 0.17$  and it has a subtle signature for  $x = 0.15$  (optimal doping). This partial gap is present in our superconducting samples in contrast to ref. [9]. The closure of the gap suggests a quantum critical point (QCP) around  $x = 0.17$ , consistent with transport evidence on similar samples [12]. We suggest that this gap originates from a spin density wave (SDW), consistent with ARPES [10], and that the QCP is an antiferromagnetic-paramagnetic one.

The thin films studied in this work were epitaxially grown by pulsed-laser deposition on a  $\text{SrTiO}_3$  substrate [13]. The samples studied are (i)  $x = 0.11$ , not superconducting down to 4 K (thickness 2890 Å), (ii)  $x = 0.13$  (underdoped)  $T_c = 15$  K (thickness 3070 Å), (iii)  $x = 0.15$  (optimally doped),  $T_c = 21$  K (thickness 3780 Å), (iv)  $x = 0.17$  (overdoped)  $T_c = 15$  K (thickness 3750 Å).  $T_c$  for all the films were obtained by electrical resistance measurements. Infrared-visible reflectivity spectra were measured for all samples in the 25–21000  $\text{cm}^{-1}$  spectral range with a Bruker IFS 66v Fourier Transform spectrometer within an accuracy of 0.2%. Data was taken at typically 12 temperatures (controlled better than 0.2 K) between 25 K and 300 K. The far-infrared (10–100  $\text{cm}^{-1}$ )

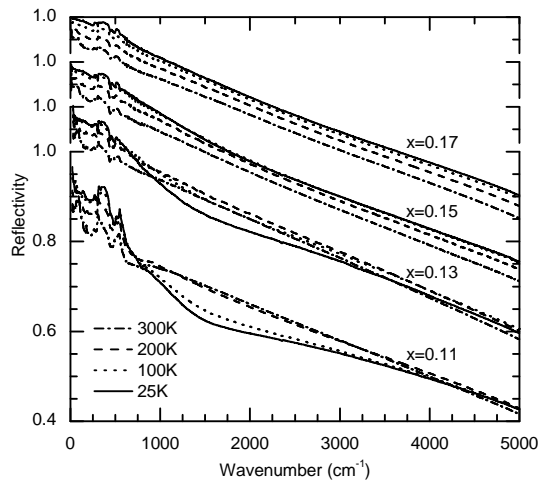


FIG. 1: Raw infrared reflectivity of  $x = 0.11, 0.13, 0.15$  and  $0.17$  samples. Curves for different concentrations are shifted from one another by  $0.1$  for clarity.

was measured for samples (iii) and (iv) utilizing a Bruker IFS 113v at Brookhaven National Laboratory.

Figure 1 shows the raw reflectivity from 25 to 5000  $\text{cm}^{-1}$  for a set of selected temperatures. As the temperature decreases, a suppression of  $R$  becomes conspicuous for  $x = 0.11$  and  $0.13$  and is visible for  $x = 0.15$  as a bending of the lowest temperature curve, crossing at 75 K. Conversely, the reflectivity of the  $x = 0.17$  sample increases monotonically with decreasing temperature over the whole spectral range shown.

We applied a standard thin film fitting procedure to extract the optical conductivity from this data set [6, 14]. The real part  $\sigma_1(\omega)$  of the optical conductivity is plotted in Fig. 2. At low energy, for all concentrations, there is a Drude-like contribution which narrows as the temperature is lowered in the normal state from 300 K to 25 K. This implies a transfer of spectral weight, from higher (above, e.g.,  $\approx 170 \text{ cm}^{-1}$  for  $x = 0.13$ ) to lower frequencies. Above 1000  $\text{cm}^{-1}$ , the feature noticed in the raw reflectivity for  $x = 0.11$  and  $0.13$  produces a dip/hump structure.  $\sigma_1(\omega)$  peaks at  $\Omega_M \sim 2750 \text{ cm}^{-1}$  for  $x = 0.11$  and at  $\sim 1500 \text{ cm}^{-1}$  for  $x = 0.13$ . A similar feature was observed in NCCO single crystals only for doping levels where such crystals are *not superconducting* [9], in contrast to our observation in the  $x = 0.13$  sample.

Homogeneity issues are a key question in cuprates [15]. We investigated the homogeneity of our samples in several ways. Using the X-ray analysis of an EDAX system, we verified that the  $x = 0.15$  sample did not present any trace of inhomogeneity on the micron scale in the Pr, Ce or Cu concentrations. We also used the standard Bruggeman effective medium approximation [16] (valid for inhomogeneities smaller than the wavelength but larger than the mean free path of  $\lesssim 50 \text{ \AA}$ ) to investigate the possibil-

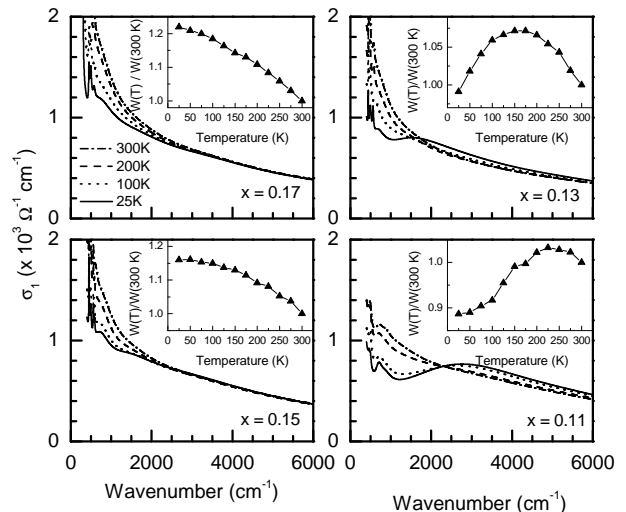


FIG. 2: Real part of the optical conductivity from 400 to 6000  $\text{cm}^{-1}$ . The inset in each panel shows the normalized spectral weight  $W(\omega_H, T)/W(\omega_H, 300 \text{ K})$  ( $\omega_L = 0$ ) plotted vs. temperature for an upper cut-off frequencies  $\omega_H = 2000 \text{ cm}^{-1}$ .

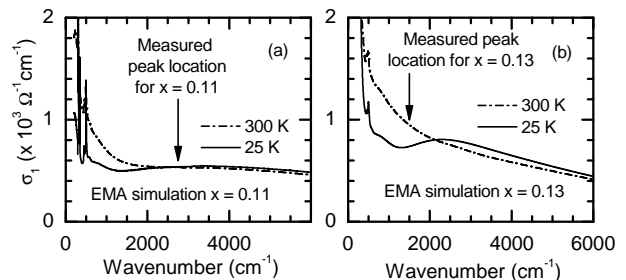


FIG. 3: Effective medium approximation (EMA) simulations of conductivity. *Left panel:* attempts to simulate  $x = 0.11$  crystal by combinations of undoped and  $x = 0.17$  conductivities. *Right panel:* attempts to simulate conductivity of  $x = 0.13$  sample by combinations of  $x = 0.11$  and  $x = 0.17$ . The proportions of each phase were chosen so that the average Ce concentration is the nominal one.

ity that the gap features observed in one concentration could arise from an inhomogeneous mixture of two different concentrations. The left hand panel of Fig. 3 shows results of an attempt to simulate the optical conductivity of the  $x = 0.11$  sample as a combination of 35%  $x=0$  [17] and 65%  $x=0.17$ , as suggested in Ref. [18]. The failure to describe the spectral weight shift and peak development is evident. The right panel of Fig. 3 shows results of an attempt to simulate the  $x = 0.13$  sample from the  $x = 0.11$  and  $x = 0.17$  ones. For no parameters were we able to place the peak in  $\sigma_1$  at the correct location. These, and other simulations (not shown) lead us to believe that the structures we observe are intrinsic.

We now present a spectral weight analysis which shows that the features seen in  $\sigma_1$  and  $R$  are due to the opening

of a partial gap. We define the restricted spectral weight  $RSW(\omega_L, \omega_H, T)$  via

$$RSW(\omega_L, \omega_H, T) = \frac{2}{\pi} \int_{\omega_L}^{\omega_H} \sigma_1(\omega, T) d\omega. \quad (1)$$

The familiar  $f$ -sum rule implies  $RSW(0, \infty, T) = ne^2/m$ ; the partial integrals provide insight into the rearrangement of the conductivity with temperature. In a conventional metal the conductivity is described by a ‘‘Drude peak’’ centered at  $\omega = 0$  and with half width  $\Gamma$  decreasing as  $T$  is lowered. In this case spectral weight is transferred from high to low energies as  $T$  decreases. On the other hand, the opening of a density wave gap leads to a transfer of spectral weight to higher energies, beyond the gap edge.

In all of our samples,  $RSW(0, 20000 \text{ cm}^{-1}, T)$  is temperature independent within 3%; however the partial integrals display an informative  $T$ -dependence. The insets to Fig. 2 display  $W(\omega_H, T) = RSW(0, \omega_H, T)$  for  $\omega_H = 2000 \text{ cm}^{-1}$ , all normalized to the  $T = 300 \text{ K}$  values. The presence of a narrow Drude peak ( $\lesssim 100 \text{ cm}^{-1}$ ) implies that accurate low frequency data (measured down to  $10 \text{ cm}^{-1}$ ) is important in order to get reliable zero-frequency extrapolations. The  $x = 0.17$  curves display the steady increase in  $W$  expected of a Drude metal. On the other hand, both the  $x = 0.11$  and  $x = 0.13$  samples display a non-monotonic behavior indicating an upward shift of spectral weight beginning below  $T \approx 225 \text{ K}$  ( $x = 0.11$ ) and  $T \approx 150 \text{ K}$  ( $x = 0.13$ ); however we note that all samples remain metallic at low temperatures as indicated by the presence of a Drude peak. In drawing this conclusion it is important to integrate down to zero to insure that the weight is not transferred downwards into a narrow Drude peak. We believe that the only consistent interpretation of these data is that as  $T$  is lowered a gap appears on *part* of the Fermi surface. In particular, simulations of two component (Drude and mid-infrared) models, such as the polaron model of Lupi *et al.* [19] leads to negligible upwards transfer of spectral weight ( $\sim 5\%$  of observed values).

To address the issue of the existence of a partial gap in the  $x = 0.15$  (optimally doped) sample we compare in Fig. 4 the  $RSW$  of  $x = 0.13, 0.15$  and  $0.17$  in two frequency ranges [*panel (a)*:  $0$  to  $500 \text{ cm}^{-1}$  and *panel (b)*:  $1000$  to  $3000 \text{ cm}^{-1}$ ]. For clarity, each curve is normalized to its value at  $300 \text{ K}$ . In both panels, the  $x = 0.17$  sample displays a monotonic evolution, as expected from the temperature dependence of its scattering rate shown in the inset. The  $x = 0.13$  sample displays a non-monotonic behavior in both frequency ranges. In panel (a) the increase of spectral weight due to the Drude narrowing is overcome at low temperatures by the gap opening. As expected, this trend is reversed in panel (b). For the  $x = 0.15$  sample, the low  $\omega$   $RSW$  [panel (a)] shows at low  $T$  ( $\lesssim 100 \text{ K}$ ) a pronounced flattening relative to the  $x = 0.17$  sample. The high  $\omega$   $RSW$  [panel (b)] shows the

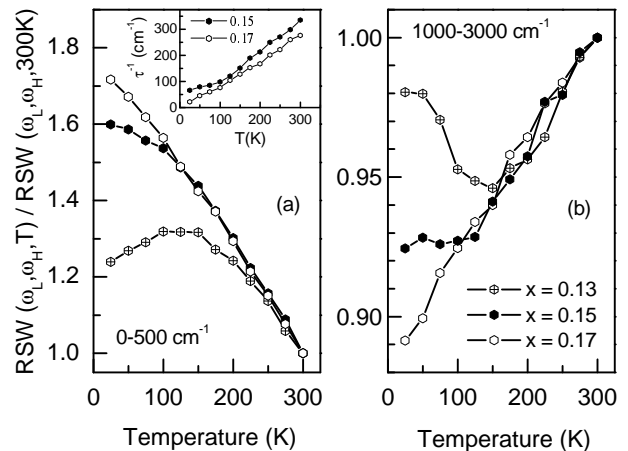


FIG. 4: Temperature evolution of the restricted spectral weight. The integration boundaries  $\omega_L$ - $\omega_H$  are indicated in each panel. The inset shows the dc extrapolation for the scattering rate for the  $x = 0.15$  and  $0.17$  samples.

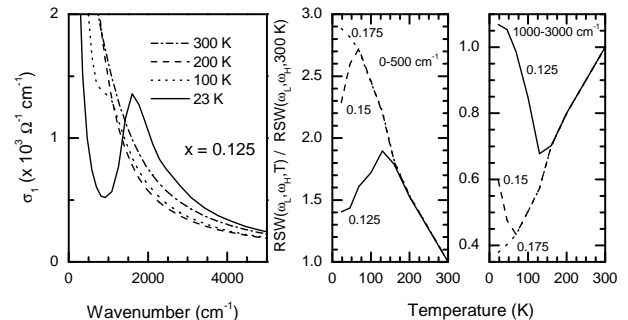


FIG. 5: *Left panel*: Optical conductivity calculated by a spin density wave model for  $x = 0.125$ . *Mid and right panels*:  $RSW$  calculated for different dopings from the spin density wave model as described in the text.

complementary effect: the decrease with decreasing  $T$  is halted below  $T \approx 100 \text{ K}$ . On the other hand, the free carrier scattering rate (inset) shows a smooth decrease over the whole temperature regime. This, combined with the clearly interpretable behavior of the  $x = 0.13$  and  $0.17$  compounds, strongly suggests that a small gap opens below  $100 \text{ K}$  for  $x = 0.15$ .

A natural interpretation is that the observed optical gap arises from commensurate  $(\pi, \pi)$  magnetic order. Neutron scattering consistent with this order has been unambiguously observed at lower dopings [20, 21, 22], but whether the order exists at superconducting concentrations is not yet settled. To investigate whether this physics can lead to the gap observed in our experiments we have calculated the optical conductivity of a theoretical model of electrons moving in a band structure defined by the tight-binding dispersion appropriate to the cuprates [23, 24] along with a  $(\pi, \pi)$  density wave gap

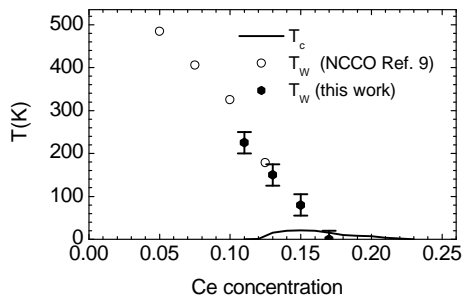


FIG. 6:  $T_c$  and  $T_W$ , the SDW (or partial) gap opening temperature (see text) versus  $x$ . Open symbols are for NCCO from ref. [9], deduced from the maximum in  $\sigma_1(\omega)$ , and using the relation  $\hbar\Omega_M/k_B T_W = 15$ .

of magnitude  $2\Delta_{SDW}$  (corresponding to the photoemission band splitting) and mean field  $T$ -dependence. Our model uses the optical matrix elements appropriate to the tight binding model and also includes a frequency and temperature dependent self energy with imaginary part increasing from a  $T$ -dependent dc limit [chosen to roughly reproduce  $\rho(T)$  at  $T < T_W$ ] to a weakly  $T$ -dependent high  $\omega$  limit. The specific form chosen is  $\Sigma(\omega, T) = i\gamma_0 + i\gamma_1 [1 - \lambda(T)\omega_c(\omega_c - i\omega)/(\omega_c^2 + \omega^2)]$  with  $\gamma_0 = 0.01$  eV,  $\gamma_1 = 0.25$  eV,  $\omega_c = 0.3$  eV and  $\lambda$  ranging from 0.7 at 300 K to 0.96 at low  $T$ . (Note that a ‘marginal Fermi liquid’ self energy would have described the data almost as well, and leads to results very similar to those presented here.) As discussed in [24] we also included frequency and matrix element rescalings, by factors  $\sim 0.6$  to account for high energy (Mott) physics. Thus the absolute values of  $\sigma$  should be regarded as estimates, but the relative frequency and temperature dependence as well as spectral weight trends are expected to be reliable. The calculated conductivity, for the doping  $x = 0.125$  and a gap which opens at 170 K and saturates at a  $T = 0$  value  $2\Delta_{SDW} = 0.14$  eV are shown in shown in the left panel of Fig. 5. The resemblance to the measured conductivity is striking. The right hand panels for Fig. 5 show representative results of the modified spectral weight analysis for three dopings [ $x = 0.125$ ,  $x = 0.15$  ( $T_W = 70$  K,  $2\Delta_{SDW} = 0.03$  eV) and  $x = 0.175$  ( $2\Delta_{SDW} = T_W = 0$ )]. The corresponding maximum in the optical conductivity occurs at  $\Omega_M \approx 2.8\Delta_{SDW}$ . It is evident that the calculation reproduces the different qualitative behaviors of the restricted spectral weight. In particular, the minimum in the high frequency  $RSW(T)$  curve corresponds to the opening of a gap. These curves therefore support the notion that the  $x = 0.15$  sample in fact has a small density wave gap, although this is not directly visible in the measured optical spectrum, and further supports that the temperature at which the gap opens may be inferred from the position of the minimum or saturation in the RSW.

Detection of the gap by other means, especially via a low energy spectroscopy which can probe the behavior as  $\Delta \rightarrow 0$  in the  $x = 0.15 - 0.17$  range, would be very desirable. Intriguing tunneling measurements [25, 26] suggest the presence of a gap which is, however, much smaller and closes at much lower temperature than the one we find.

Figure 6 shows the gap onset temperature  $T_W$  obtained from the breakpoints in Figs. 2 and 4, along with those extracted from Onose *et al.* [9] as a function of Ce concentration. Our work, covering a larger doping range up to the overdoped regime, strongly suggests that the  $T_W$  line ends at a critical concentration of  $x \sim 0.17$ . This supports the arguments, obtained from dc transport in similar samples [12], and strongly suggests that the QCP is of magnetic origin.

In conclusion, we have measured with great accuracy the reflectivity of electron doped  $\text{Pr}_{2-x}\text{Ce}_x\text{CuO}_4$  at various Ce doping levels ( $x$ ). A careful optical conductivity spectral weight analysis shows that a partial gap opens below a temperature  $T_W$  up to Ce concentrations of  $x = 0.15$ . A spin density wave model reproduces satisfactorily the data where the gap has a clear spectral signature (for example  $x = 0.13$ ). The gap magnitude  $2\Delta_{SDW}$  relates to  $T_W$  through  $2\Delta_{SDW}/k_B T_W \sim 11$ .  $T_W$  extrapolates to zero for  $x \sim 0.17$ , suggesting the presence of a quantum critical point inside the superconducting dome. We have shown that, in at least one class of high- $T_c$  superconductors, a ‘pseudogap’ is associated with an ordered phase terminating in a QCP at approximately optimal doping. We hope these results will provide a point of reference which will help to resolve similar issues arising in the hole-doped materials.

The authors thank Dr. V.N. Kulkarni for RBS / Channeling measurements and Dr. P. Bassoul for electronic microscopy studies. The work at University of Maryland was supported by NSF grant DMR-0102350. The work at Columbia was supported by NSF contract DMR-0338376. The Work at Brookhaven National Laboratory as supported by DOE under contract DE-AC02-98CH10886.

\* Electronic address: lobo@espci.fr

- [1] P. Fournier *et al.*, in *The Gap Symmetry and Fluctuations in High- $T_c$  Superconductors*, edited by J. Bok (Serie B: Physics Vol.371, NATO ASI Series, 1998).
- [2] H. Alloul, T. Ohno and P. Mendels, *Phys. Rev. Lett.* **63** 1700 (1989).
- [3] M. Takigawa *et al.*, *Phys. Rev.* **B43** 247 (1991).
- [4] M.N. Norman *et al.*, *Nature* **392**, 157 (1998).
- [5] A.V. Puchkov, D.N. Basov, and T. Timusk, *J. Phys. Condens. Matter* **8**, 10049 (1996).
- [6] A.F. Santander-Syro *et al.*, *Phys. Rev. Lett.* **88**, 097005 (2002).
- [7] C.C. Homes *et al.*, *Phys. Rev. B* **56**, 5525 (1997).

- [8] E.J. Singley *et al.*, Phys. Rev. B **64**, 224503 (2001).
- [9] Y. Onose *et al.*, Phys. Rev. B **69**, 024504 (2004).
- [10] N.P. Armitage *et al.*, Phys. Rev. Lett. **88**, 257001 (2002).
- [11] A. Zimmers *et al.*, condmat/0405284.
- [12] Y. Dagan *et al.*, Phys. Rev. Lett. **92**, 167001 (2004).
- [13] E. Maiser *et al.*, Physica C **297**, 15 (1998).
- [14] A.F. Santander-Syro *et al.*, condmat/0405264.
- [15] K. McElroy *et al.* Nature **413**, 282 (2001).
- [16] P. Wissmann and R.E. Hummel, *in* Handbook of optical properties. Vol. 2, edited by CRC Press (1997).
- [17] C. C. Homes *et al.*, Phys. Rev. B **66**, 144511 (2002).
- [18] T. Uefuji *et al.*, Physica C **392-396**, 189 (2003).
- [19] S. Lupi *et al.*, Phys. Rev. Lett. **83**, 4852 (1999).
- [20] T.R. Thurston *et al.*, Phys. Rev. Lett. **65**, 263 (1990).
- [21] M. Matsuda *et al.*, Phys. Rev. B **45**, 12548 (1992).
- [22] K. Yamada *et al.*, J. Phys. Chem. Sol. **60**, 1025 (1999).
- [23] O.K. Andersen, cond-mat/9509044
- [24] A.J. Millis and H.D. Drew, Phys. Rev. B **67**, 214517 (2003).
- [25] A. Biswas *et al.*, Phys. Rev. B **64**, 104519 (2001).
- [26] L. Alff *et al.* Nature **422**, 698 (2003).